Article

Cell

Inhibiting DNA Methylation Causes an Interferon Response in Cancer via dsRNA Including Endogenous Retroviruses

Graphical Abstract

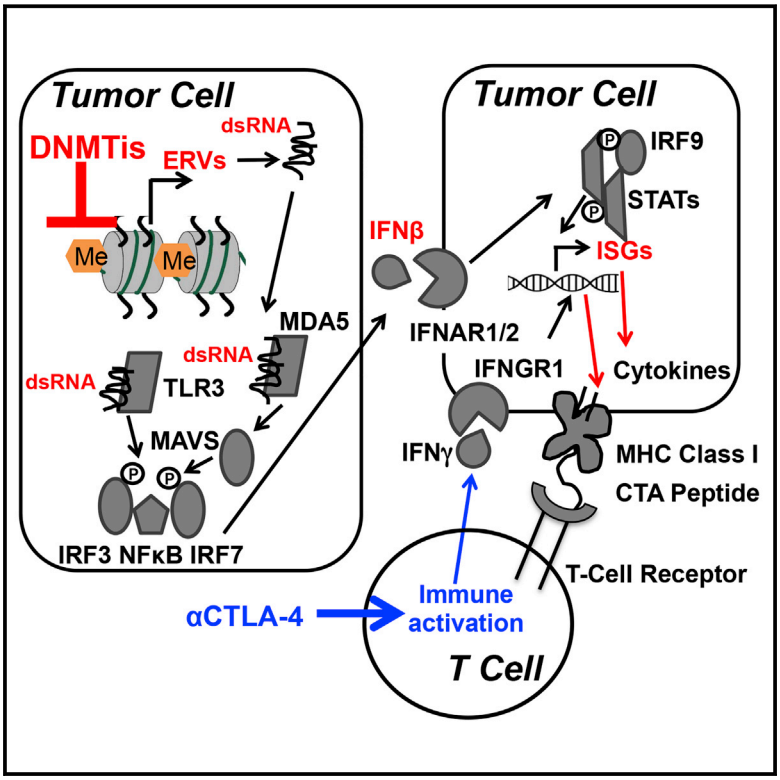

Highlights

- DNMTis induce an interferon response in cancer cells by activating dsRNA sensors
- DNMTis induce ERV demethylation and expression helping trigger the dsRNA response
- DNMTi viral defense genes in melanoma track with patient response to immune therapy
- DNMTi treatment sensitizes to anti-CTLA-4 immunotherapy in a melanoma mouse model

Authors

Katherine B. Chiappinelli, Pamela L. Strissel, Alexis Desrichard, ..., Timothy A. Chan, Stephen B. Baylin, Reiner Strick

Correspondence

sbaylin@jhmi.edu (S.B.B.), reiner.strick@uk-erlangen.de (R.S.)

In Brief

DNA methyltransferase inhibitors upregulate endogenous retroviruses in tumor cells to induce an growth-inhibiting immune response. High expression of the genes associated with the anti-viral response seems to potentiate a response to immune checkpoint therapy.

Chiappinelli et al., 2015, Cell *162*, 974–986
August 27, 2015
http://dx.doi.org/10.1016/j.cell.2015.07.011

CellPress

Cell

Article

Inhibiting DNA Methylation Causes an Interferon Response in Cancer via dsRNA Including Endogenous Retroviruses

Katherine B. Chiappinelli,[1,7] Pamela L. Strissel,[2,7] Alexis Desrichard,[3,7] Huili Li,[1] Christine Henke,[2] Benjamin Akman,[1] Alexander Hein,[2] Neal S. Rote,[4] Leslie M. Cope,[1] Alexandra Snyder,[3,5] Vladimir Makarov,[3] Sadna Buhu,[5] Dennis J. Slamon,[6] Jedd D. Wolchok,[5] Drew M. Pardoll,[1] Matthias W. Beckmann,[2] Cynthia A. Zahnow,[1] Taha Merghoub,[5,8] Timothy A. Chan,[3,5,8] Stephen B. Baylin,[1,8,*] and Reiner Strick[2,8,*]

[1]Department of Oncology, The Sidney Kimmel Comprehensive Cancer Center at Johns Hopkins, Baltimore, MD 21287, USA
[2]Department of Gynaecology and Obstetrics, Laboratory for Molecular Medicine, University-Clinic Erlangen, 91054 Erlangen, Germany
[3]Human Oncology and Pathogenesis Program, Memorial Sloan Kettering Cancer Center, New York, NY 10065, USA
[4]Department of Reproductive Biology, Case Western Reserve University, Cleveland, OH 44106, USA
[5]Department of Medicine, Memorial Sloan Kettering Cancer Center, New York, NY 10065, USA
[6]The Jonsson Comprehensive Cancer Center, University of California-Los Angeles, Los Angeles, CA 90095, USA
[7]Co-first author
[8]Co-senior author
*Correspondence: sbaylin@jhmi.edu (S.B.B.), reiner.strick@uk-erlangen.de (R.S.)
http://dx.doi.org/10.1016/j.cell.2015.07.011

SUMMARY

We show that DNA methyltransferase inhibitors (DNMTis) upregulate immune signaling in cancer through the viral defense pathway. In ovarian cancer (OC), DNMTis trigger cytosolic sensing of double-stranded RNA (dsRNA) causing a type I interferon response and apoptosis. Knocking down dsRNA sensors TLR3 and MAVS reduces this response 2-fold and blocking interferon beta or its receptor abrogates it. Upregulation of hypermethylated endogenous retrovirus (ERV) genes accompanies the response and ERV overexpression activates the response. Basal levels of ERV and viral defense gene expression significantly correlate in primary OC and the latter signature separates primary samples for multiple tumor types from The Cancer Genome Atlas into low versus high expression groups. In melanoma patients treated with an immune checkpoint therapy, high viral defense signature expression in tumors significantly associates with durable clinical response and DNMTi treatment sensitizes to anti-CTLA4 therapy in a pre-clinical melanoma model.

INTRODUCTION

DNA methyltransferase inhibitors (DNMTis) such as 5-azacytidine (Aza) and 5-aza-2′-deoxycytidine (Dac) are effective cancer therapies in hematologic neoplasms (Issa, 2005; Matei et al., 2012) and are Food and Drug Administration (FDA)-approved for the pre-leukemic disorder myelodysplasia (MDS) (Kaminskas et al., 2005). These cytidine analogs incorporate into DNA, block catalytic actions of DNA methyltransferases (DNMTs), and trigger their degradation (Stresemann et al., 2006). Preclinically, low doses avoid early cytotoxicity and DNA damage, allowing cells to exhibit apparent reprogramming and blunting of tumorigenicity (Tsai et al., 2012). Mechanisms can include reversal of abnormal promoter DNA methylation, re-expression of silenced genes including tumor suppressors (Baylin and Jones, 2011), and changes to cancer signaling pathways including apoptosis, cell-cycle activity, and stem cell functions (Tsai et al., 2012).

A long recognized activity of DNMTis described by others (Karpf et al., 1999, 2004) and our group (Li et al., 2014; Wrangle et al., 2013), is induction of immune responses in cancer cells. In recent clinical trials for non-small cell lung cancer (NSCLC) (Juergens et al., 2011; Wrangle et al., 2013) a small number of patients had remarkably robust and durable responses to immune checkpoint blockade therapy after first receiving Aza (Wrangle et al., 2013). This immune therapy alone also has activity against NSCLC (Brahmer et al., 2010, 2012; Topalian et al., 2012). A larger trial is now ongoing to determine if Aza can indeed prime patients for sensitization to checkpoint inhibition (Brahmer, 2015). For NSCLC and other tumor types, Aza induces interferon signaling and concordant upregulation of surface antigens and their assembly proteins, viral defense pathways, and transcript and surface protein levels of PD-L1, the key checkpoint ligand targeted in the above immunotherapy (Li et al., 2014; Wrangle et al., 2013). Indeed, we have defined a 300-gene expression signature we termed Aza-induced immune genes or AIM (Li et al., 2014) for which activation is greatest for epithelial ovarian cancer (EOC) and NSCLC (Li et al., 2014). Genome-wide expression of AIM separates primary EOC, NSCLC, and other cancers into high and low expression groups (Li et al., 2014). We hypothesize the low group may represent an ''immune evasion/immune editing'' pattern (Drake et al., 2006; Schreiber et al., 2011) that Aza could reverse to sensitize patients to subsequent immune therapy (Li et al., 2014).

We now show that a major mechanism underlying the Aza-triggered immune response is induction of a cytosolic

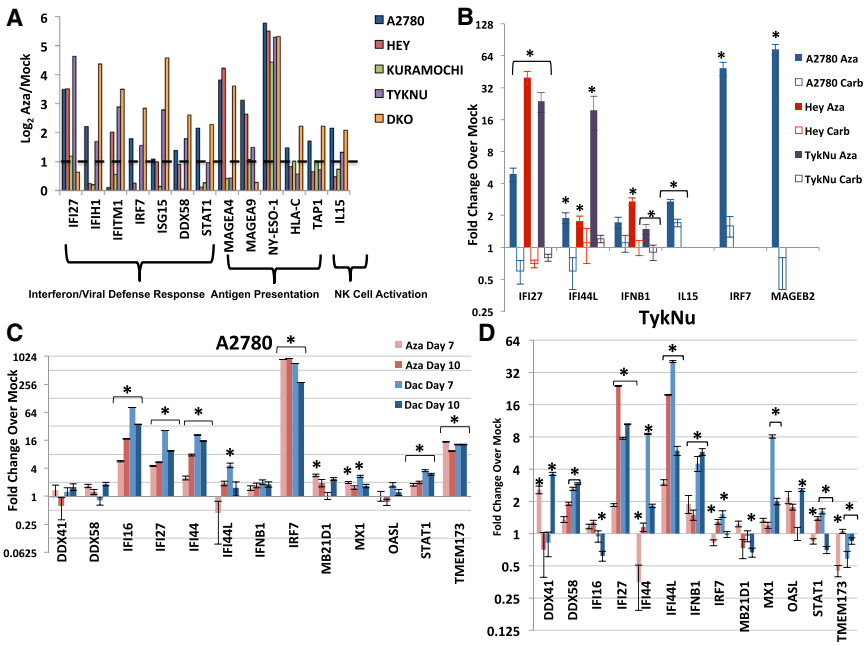

Figure 1. DNMT Inhibitors Upregulate Immune Genes in Ovarian Cancer Cell Lines

(A) Levels of immune genes in four EOC cell lines and DKO colon cancer cell line (DNMT1$^{-/-}$, DNMT3B$^{-/-}$) relative to its parental HCT116 line. y axis, $\log_2$ Aza/Mock fold change from microarray data. Dotted line denotes 2-fold change.

(B) qRT-PCR validation of immune genes in EOC cells treated for 72 hr: Mock, 500 nM Aza, or 500 nM- 3 μM carboplatin and rested for 7 days before assaying (day 10). IC_{50}s were A2780 (Aza, 848 nM; Carb, 457 nM), Hey (Aza, 4.1 μM; Carb, 12.2 μM), TykNu (Aza, 491 nM; Carb, 986.2 nM).

(C and D) qRT-PCR validation of interferon response genes in the A2780 (C) and TykNu (D) EOC lines treated with no drug (Mock), 500 nM Aza (Aza), or 100 nM Decitabine (Dac) for 3 days, and rested for 4 (day 7) or 7 (day 10) days before assaying. Data in (B)–(D) are represented as mean ± SEM of three biological replicates, y axis = fold change over mock. *p ≤ 0.05.

See also Figure S1.

double-stranded RNA (dsRNA) sensing pathway used by epithelial and other cell types as a viral defense mechanism that triggers a type I interferon response (Kulaeva et al., 2003; Sistigu et al., 2014). A key contributor is induction of increased expression of multiple DNA hypermethylated endogenous retroviruses (ERVs). In The Cancer Genome Atlas (TCGA), the viral defense gene expression separates primary EOC and other cancers into high and low expression and high tumor expression strongly associates with clinical benefit in a trial of immune checkpoint therapy for advanced melanoma. Aza sensitizes to immune checkpoint blockade in a pre-clinical model of melanoma. We thus define a potential approach in which an epigenetic therapy may sensitize cancer cells to various immunotherapies.

RESULTS

DNMTis Trigger Viral Defense and Type I Interferon Signaling

Induction of AIM in a previous study of 23 EOC cell lines (Li et al., 2014) included, in addition to previously reported DNA hypermethylated cancer testis antigens (*MAGEA4, MAGEA9, NY-ESO-1*) (James et al., 2013; Karpf et al., 2004, 2009; Odunsi et al., 2014), interferon/viral defense, antigen processing and presentation, and host immune cell attraction genes (Figure 1A). Direct Aza targeting of DNMTs for these changes is suggested by similar findings in DKO colon cancer cells genetically disrupted for two major DNMTs (*DNMT1*$^{-/-}$, *DNMT3B* $^{-/-}$) versus parental, wild-type HCT116 cells (Figure 1A). The induced responses may not be a general stress phenomenon as they did not occur with carboplatin, a cytotoxic agent commonly used in EOC treatment (Figure 1B). Aza and Dac incorporate into DNA, inhibiting three DNA methyltransferases, but Aza also incorporates into RNA, inhibiting the RNA methyltransferase DNMT2 (Schaefer et al., 2009). Aza thus can demethylate RNA, and unmethylated RNA may activate TLR3 and the interferon response (Karikó et al., 2005). However, Dac and Aza both mimicked the DKO cell line results (Figures 1A, 1C, 1D, S1A, and S1B) strongly suggesting that the drugs directly target DNA methylation to trigger the interferon response.

Aza and Dac similarly triggered an interferon response that includes interferon beta (*IFNβ1*) and a panel of interferon-stimulated genes (ISGs) (*IFI16*, *IFI27*, *IFI44*, *IFI44L*, *MX1*, and *OASL*) (Figures 1C, 1D, S1A, and S1B). Each ISG functions predominantly in anti-viral and anti-proliferative signaling (Figure 2A; Ivashkiv and Donlin, 2014). In four EOC cell lines, key upstream genes in the type I Interferon pathway (*IFNβ1*, *IRF7*, and *STAT1*) were generally upregulated at the fourth day following the end of Aza treatment ("day 7") and further increased by day 10 (Figures 1C, 1D, S1A, and S1B). Importantly, cytosolic sensors for DNA (*MB21D1*/CGAS and *TMEM173*/STING) and RNA (*DDX41*, *DDX58*/RIG-I, and *IFIH1*/MDA5) were also variably upregulated (Figures 1A, 1C, 1D, S1A, and S1B). In A2780 and TykNu, but not Hey or Kuramochi, cell lines, variable increases occurred in type III interferon signaling genes, also involved in response to viruses (Ding and Robek, 2014). These included *IFNL1* (IL28A) and *IFNL3* (IL29) ligands (Figure S1C) and especially the IFN III receptor *IFNLR1* (Figure S1C), known to be methylated and activated by epigenetic therapy (Ding et al., 2014).

Key viral RNA sensing proteins include TLR3 on the endosomal membrane and MDA5, PKR, and RIG-I in the cytoplasm (Figure 2A). These induce IRF3, IRF7, and NF-κB to translocate to the nucleus and activate transcription of *IFNβ1* (Ivashkiv and Donlin, 2014). *IRF7* is frequently promoter DNA hypermethylated in cancer and the associated low basal expression can be reversed by Aza in squamous NSCLC (Wrangle et al., 2013). Among 23 EOC lines examined, *IRF7* was hypermethylated in only one, A2780 (Li et al., 2014) (Figure S3A), potentially not a classic high-grade EOC (Anglesio et al., 2013;

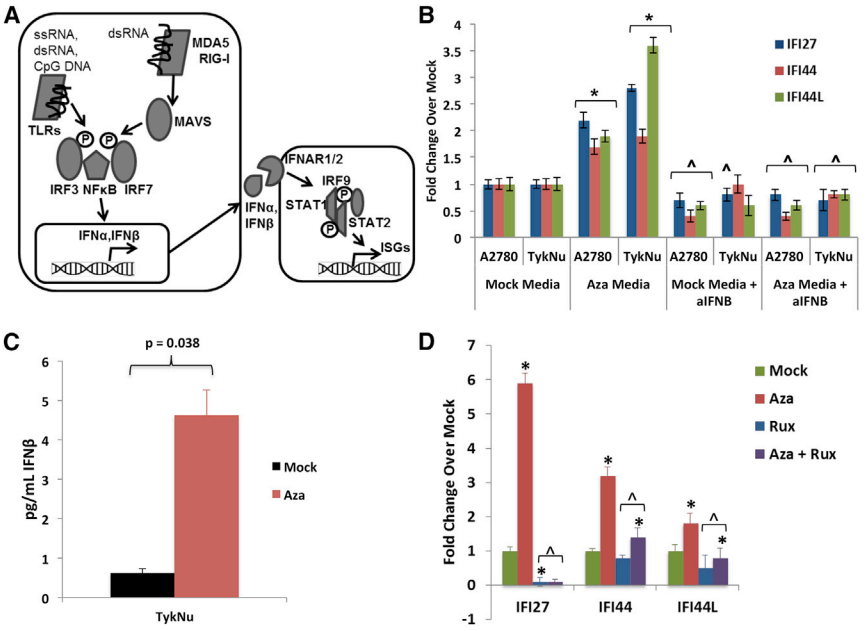

Figure 2. DNMTis Upregulate Immune Signaling through Secreted Interferon

(A) Schematic of interferon pathway. Protein symbols outlined in text.

(B) Treatment of recipient A2780 or TykNu cells with media from cells treated with Mock or Aza, +/− addition of anti-IFNβ. y axis, qRT-PCR fold Aza/Mock of ISGs. *$p \leq 0.05$ and ^$p \leq 0.05$, respectively, for Mock or Aza media with versus without anti-IFNβ versus Mock or Aza media plus anti-IFN β.

(C) ELISA of IFNβ in media from TykNu cells at day 10 from studies in (B). y axis, pg/mL IFNβ.

(D) Treatment of EOC cells with Aza as in Figures 1C and 1D, but in the presence of 2 μM Ruxolitinib (Rux). y axis, qRT-PCR fold changes for ISGs. *$p \leq 0.05$ for fold Aza over Mock and ^$p \leq 0.05$, Mock or Aza versus Mock + Rux or Aza + Rux. Data, mean ± SEM of three (B and D) or four (C) biological replicates.

See also Figure S2.

Domcke et al., 2013). Aza induced partial *IRF7* demethylation and increased expression in this cell line at days 7 and 10 while carboplatin did not (Figures 1B, 1C, and S3A), and *IRF7* knockdown significantly reduced the Aza interferon response (Figures S3B and S3C). Such *IRF7* induction did not occur in two EOC lines or the HCT116 colon cancer cell line where the gene is not hypermethylated (Figures 1D, S1A, S1B, and S3A).

When *IRF7* is not silenced, other mechanisms must then be operative for Aza to trigger viral defense signaling. Secreted IFNβ is critical to this signaling and, through interaction with surface receptors IFNAR1/2, activates JAK/STAT signaling, transcription of ISGs, and resultant translation inhibition and apoptosis (Platanias, 2005; Ivashkiv and Donlin, 2014) (Figure 2A). Indeed, media transferred to untreated cells from Aza-treated cells 7 days after drug withdrawal caused an interferon response with increased expression of ISGs *IFI27*, *IFI44*, and *IFI44L* (Figure 2B). Moreover, Aza treatment induced secreted IFNβ in media (Figures 2C and S2A) and an IFNβ blocking antibody significantly blocked the Aza-induced ISG media response (Figure 2B). Like type I IFN signaling, type III IFN signaling can be activated by viral infection (Robek et al., 2005; Ding and Robek, 2014). However, even though we observed upregulation of type III ligand transcripts *IFNL1* (IL28A) and *IFNL3* (IL29) (Figure S1C), secreted type III interferon proteins were undetectable by ELISA (Figure S2B).

Aza appears to activate type I, IFNβ-mediated signaling through JAK/STAT, as the JAK/STAT inhibitor ruxolitinib strongly reduced ISG responses (Figures 2D and S2C). Further, antibody blocking of IFNAR2, the IFNβ receptor, abrogated Aza induction of *IFI27*, *IFI44L*, and *IFI6* transcription (Figures 3A and S2D), as did inhibition of IFNβ itself (Figures 3B and S2E). In contrast, blocking the type III interferon, IL10RB receptor, gave only a modest block of *IFI27* increase (Figure S2F). IFNβ binding to IFNAR2 also may contribute to late, Aza-induced apoptosis that peaks at 4–7 days after Aza withdrawal, since anti-IFNAR2 led to a lower ratio of cleaved/total PARP (Figures 3A, 3C, and S2D and S2G).

DNMTis Trigger Viral Defense through Induction of dsRNA

Aza-induced viral defense genes and *IFNβ1* are not generally DNA methylated at promoter regions (Li et al., 2014), thus Aza may activate the pathway upstream of these genes. We considered increases in dsRNA, viral single-stranded RNA (ssRNA), and unmethylated CpG DNA that might trigger cytosolic sensors (Sun et al., 2013). Indeed, 3 days after ending Aza treatment of A2780 and TykNu ovarian cancer cells and subsequent transfection into HT29 colon cancer cells, known to have a robust interferon response (Chiappinelli et al., 2012), cytoplasmic total RNA (without rRNA) and PolyA$^+$ RNA, but not PolyA$^-$ RNA or DNA, increased *IFNβ1* transcripts (Figure 3D) and downstream ISGs (Figures 3E and S3D). Further, RNaseIII treatment of the cytosolic nucleic acids, which specifically digests dsRNA, eliminated the *IFNβ1* upregulation (Figure 4A), but this was not seen with RNaseH treatment that digests DNA-RNA hybrids (Figure S4A).

If dsRNA is required for the above Aza effects, then the key cytosolic sensors, TLR3, MDA5 (*IFIH1*), and RIG-I (*DDX58*), the latter two signaling through the mitochondrial protein, MAVS, should be involved in subsequent *IFNβ1* induction (Figure 2A). Aza increased transcript (Figure 1A) and protein levels for these (Figure 4B). However, RIG-I, which requires a 5′ triphosphate group on RNA for activation, is likely not a key player since alkaline phosphatase treatment of cytosolic nucleic acid fractions did not abolish *IFNβ1* upregulation (Figure S4D). In contrast, knockdown of TLR3 and MAVS in A2780 cells (Figure 2A) decreased Aza upregulation of interferon genes *IFNB1*, *IFI44*, *IFI44L*, and *IFI27* by 2-fold as did MAVS knockdown (Figures 4C, 4D, and S4B). In TykNu, knockdown of TLR3 and MAVS significantly blunted Aza induction of these gene responses

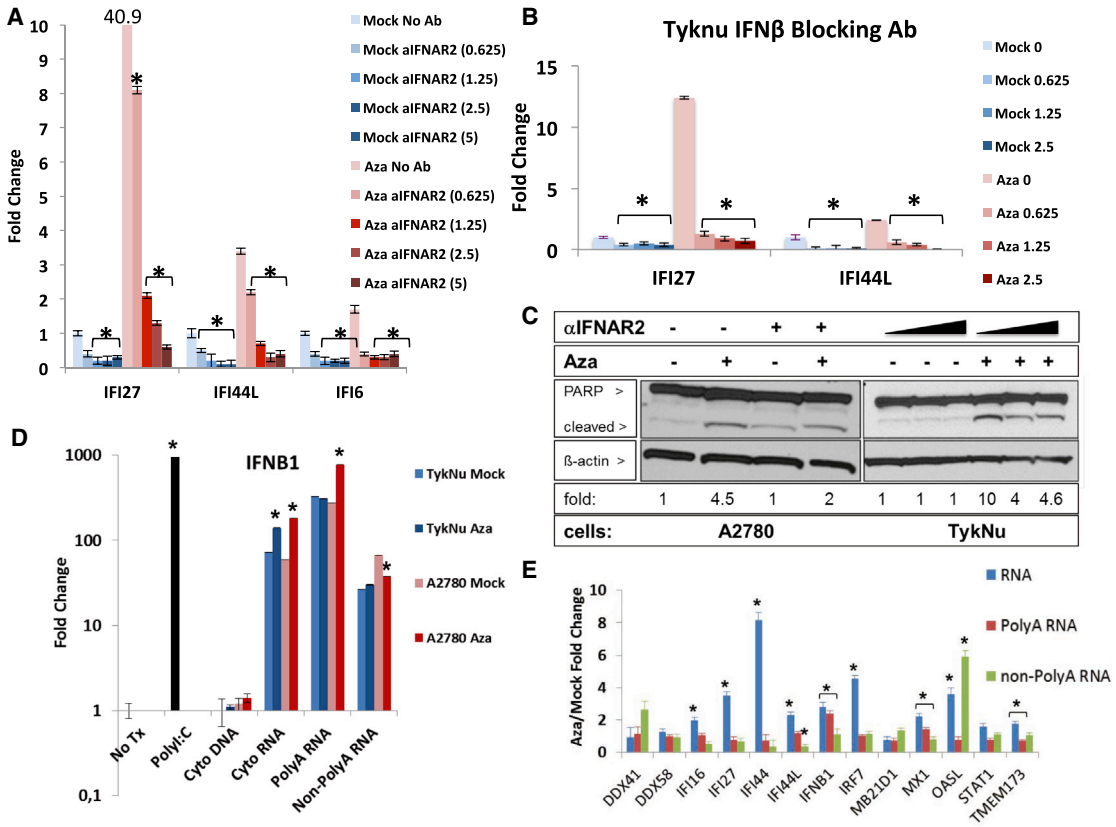

Figure 3. Aza Induces Immune Signaling through dsRNA Activation of Secreted Interferon

(A and B) Blocking (A) IFNAR2 (αIFNAR2) or (B) IFNβ in TykNu cells treated versus non-treated with Aza as in Figures 1C and 1D; parentheses, U/ml of antibody. y axis, qRT-PCR for ISGs. *p ≤ 0.05 for (A), Mock or Aza −anti-IFNAR2 versus +anti-IFNAR2, (B) Mock or Aza with no anti-IFNβ versus with anti-IFNβ.

(C) Immunoblotting for cleaved PARP with β-actin loading control. Fold change shown for cleaved/total PARP ratio, normalized to β-actin for each dose of anti-IFNAR2 (triangles, 0–1.25 U/ml). Aza compared to Mock = 1. The A2780 and TykNu cell lysates were run on two separate gels to perform western blots. The space in between the PARP and B-Actin proteins was cropped out to conserve space.

(D and E) Indicated nucleic acids from the cytoplasm of A2780- or TykNu-treated cells with no drug (Mock) or 500 nM Aza (Aza) for 3 days and rested without drug for 4 days before transfection into recipient HT29 cells. y axis, fold change, Aza/Mock, for *IFNβ1* transcript (D) or ISG transcripts (E) induced in HT29s. No Tx, no transfection; Cyto DNA, cytoplasmic DNA; Cyto RNA, cytoplasmic RNA excluding rRNA. *p ≤ 0.05 for (D) fold change Aza versus Mock, (E) Aza/Mock. Data in (A), (B), (D), and (E) are mean ± SEM of three biological replicates.

See also Figure S3.

(Figure S4C). Importantly, knock down of STING, the cytosolic DNA sensor (Mankan et al., 2014) did not blunt Aza-induced interferon signaling (Figures 4C and 4D). A previous report had implicated STING in viral cytosolic sensing in B cells, but this was dependent upon viral reverse transcriptase activity, likely to be low in our cells (Mankan et al., 2014). We thus conclude that MAVS and TLR3 are centrally involved in Aza triggering cytosolic sensors to induce an interferon response.

Aza-Induced Human Endogenous Retrovirus Transcripts Can Activate Viral Defense Responses in EOC

The above data suggests Aza might activate endogenous retroviral sequences (ERVs) that constitute more than 8% of the human genome, can activate cytosolic RNA sensors, and are silenced in normal somatic cells by promoter DNA methylation (Bannert and Kurth, 2004; Tristem, 2000; Hurst and Magiorkinis, 2014; Mankan et al., 2014). Some cancers lose ERV DNA methylation and aberrantly overexpress ERVs (Larsen et al., 2009; Rycaj et al., 2015; Strick et al., 2007; Strissel et al., 2012; Wang-Johanning et al., 2001, 2007) while others maintain silencing. Aza can induce specific ERV transcripts in melanoma, choriocarcinoma, and endometrial cancer cells (Laska et al., 2013; Ruebner et al., 2013; Stengel et al., 2010; Strissel et al., 2012). Indeed, in initial testing, the *ERVK* subfamily (Wang-Johanning et al., 2003) transcripts increased 2.5-fold in the A2780 cell line upon Aza treatment (data not shown). Upregulation of individual ERVs (22 full-length *env*, 6 partial coding *env*, 1 full-length *gag*, and 2 partial coding *pol*s) (Tables S1 and S2), in PCR assays for non-repeat sequences, occured especially at day 7 (coinciding with ISG expression) in three EOC lines following Aza and Dac treatment (Figures 5A, 5B, and S5A–S5C). These included several known ERV *env* genes like *Syncytin-1*, *ERV-3*, *env-K*, and *env-H* (Blond et al., 1999; Löwer

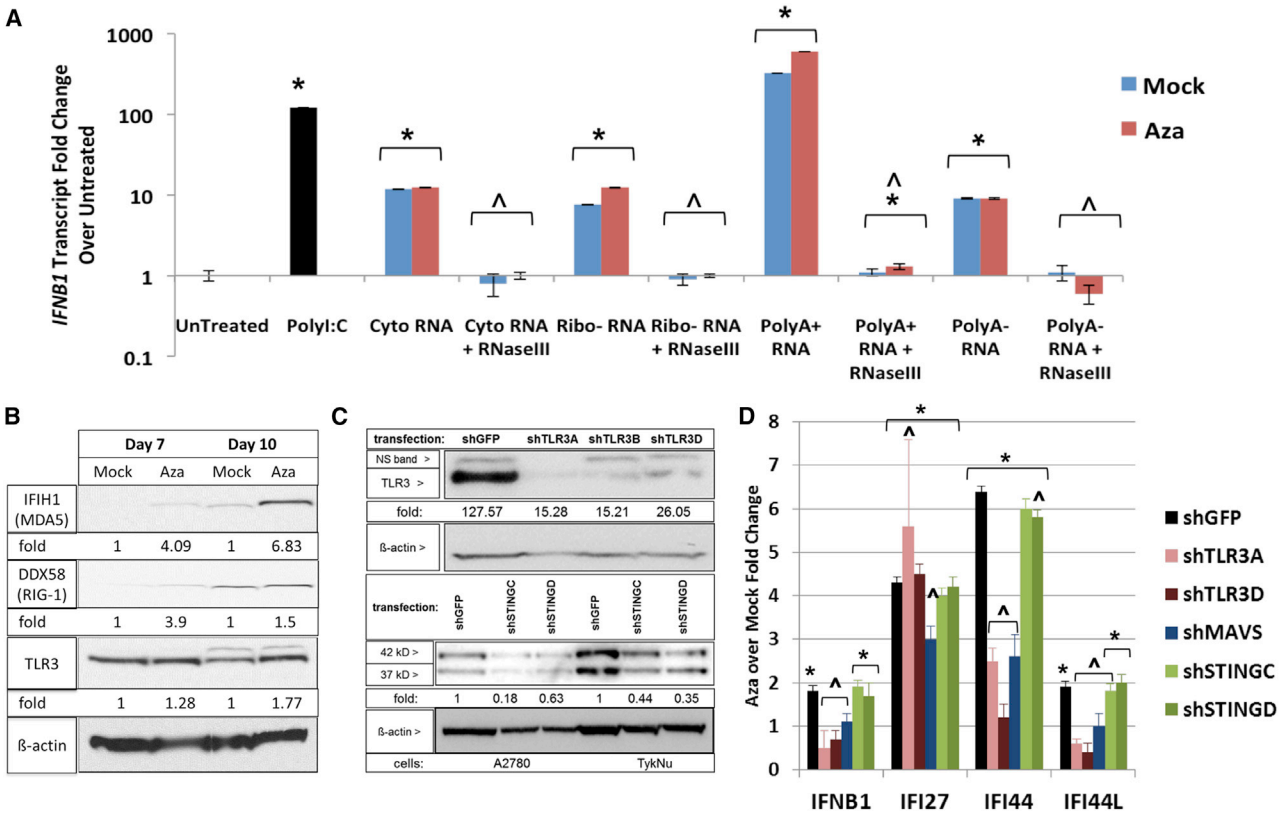

Figure 4. Aza Activates dsRNA Sensors to Induce Interferon Signaling

(A) Effects on *IFNβ1* transcripts, at 24 hr, in HT29 recipient cells transfected with nucleic acid fractions, treated with RNaseIII, from A2780 as in Figures 3D and 3E. *IFNβ1* transcripts were measured at 24 hr. y axis = IFNB1 fold change, *$p \leq 0.05$ for fold change over untreated; ^$p \leq 0.05$ for Mock or Aza + versus − RNaseIII.

(B) Western blots for MDA5, RIG-I, and TLR3 in A2780 cells at four (day 7) and seven (day 10) days after Mock versus 500 nM Aza (Aza) for 3 days. The same A2780 lysate gel was blotted for MDA5 and β-actin, then stripped and reprobed for RIG-I and TLR3. The space between the MDA5, RIG-I, and TLR3 and β-actin proteins was cropped out to conserve space.

(C) Knockdown upon lentiviral infection, with puromycin selection, of A2780 and TykNu with shGFP, shTLR3, and shSTING hairpins. Immunoblotting with anti-TLR3, anti-STING, and anti-β-actin. Densitometry fold change, normalized to mock or shGFP, shown at the bottom of the gels. The shTLR3 and shSTING cell lysates were run on two separate gels to perform western blots. The space in between the TLR3 and β-actin proteins was cropped out to conserve space. The STING western blot was stripped and reprobed with β-actin as a loading control.

(D) qRT-PCR for ISGs from (B) and (C). *$p \leq 0.05$ Aza over Mock; ^$p \leq 0.05$ shGFP versus each shRNA sensor with mean fold change ± SEM of three biological replicates.

See also Figure S4.

et al., 1993; Mi et al., 2000; Rote et al., 2004) and at especially high levels, *env-Fc2*, a less well-characterized gene (Bénit et al., 2003). Finally, in DKO as well as Aza-treated A2780 and TykNu cells, loss of *env-Fc2* promoter methylation correlated with increased *Fc2* expression (Figures 5B, 6A–6C, and S6A) but not in Hey cells (Figure S6A).

Further linking ERVs with a dsRNA-triggered IFN response, bidirectional transcription producing sense and anti-sense transcripts occurred for *Syncytin-1* and five *env-Fc2* gene loci, but not β-actin, in three EOC lines and HCT 116 and DKO cells (Figure 5C; Table S2), analyzed by the TAG-aided sense/antisense transcript detection (TASA-TD) technique (Henke et al., 2015). Such sense and antisense transcripts can form dsRNA (Faghihi et al., 2008; Su et al., 2012). Interestingly for TykNu, there was a 6.69-fold increase of *env-Fc2* antisense transcript levels compared to the sense transcript (Figure 5C) but substantially lower antisense transcripts were seen in both HCT116 and DKO cells (Figures 5C and 6A). Disrupting DNMTs seems integral to the above ERV upregulation since increases of *env-Fc2* and *erv9-1* occurred in DKO versus wild-type HCT116 cells (Figure 6A).

ERV transcripts seem directly involved in the Aza responses that, first, although drug-induced upregulation of ERV transcripts began early after Aza, both ERVs and viral defense gene increases generally peaked by day 7 (Figures S6D and S6J). Second, ERV env proteins such as Syn1 and ERV-3 were not increased after Aza treatment, supporting a dominant role for viral defense signaling via RNA transcripts (Figures 6D, S6B, and S6C). Third, overexpression of *ERV-3*, *EnvW2*, and *Syncytin-1* in TykNu (Figures 6E and 6J), A2780 (Figure S6D), and Hey cells (Figures S6E and S6J), as compared to control genes, increased the same interferon genes induced by Aza (*IFNβ1*,

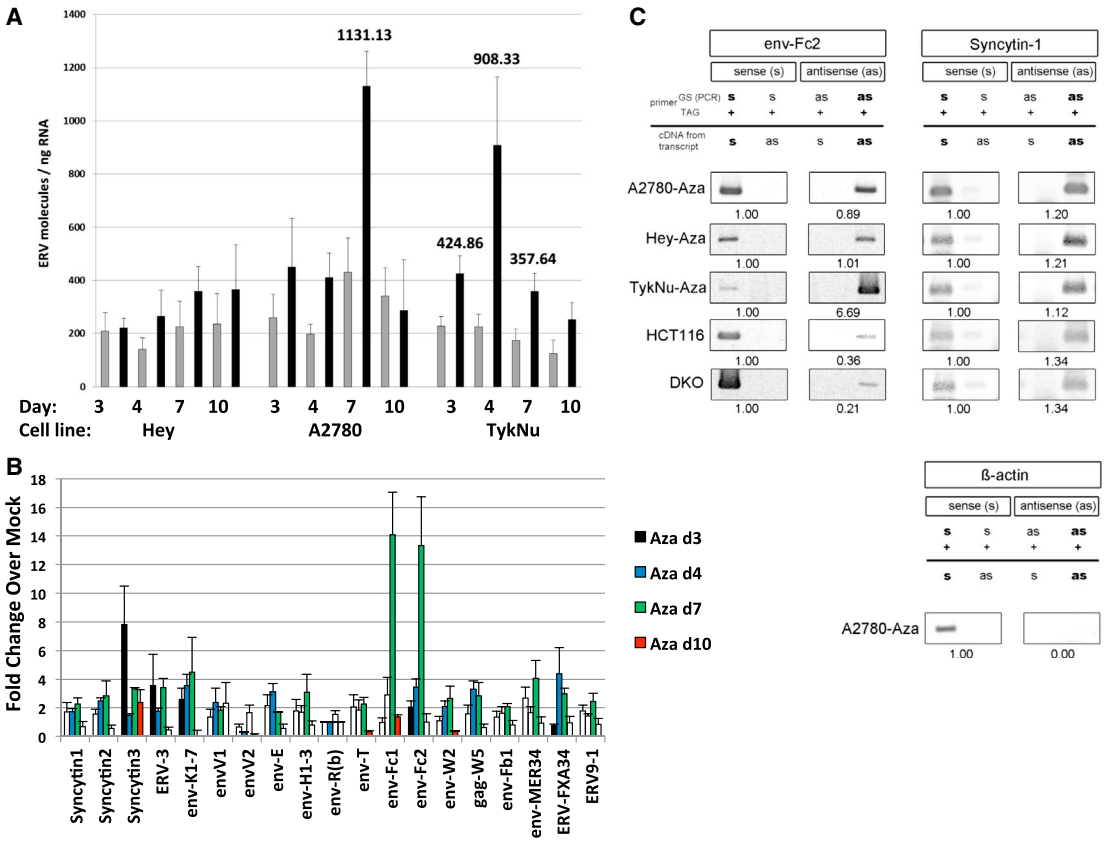

Figure 5. Aza Upregulates Sense and Antisense ERV Transcripts

RNA was isolated from cells at last (day 3), one (day 4), three (day 7), and seven (day 10) days after Mock or 500 nM Aza (Aza) for 3 days.

(A) Total number of molecules for all ERV genes (y axis = ERV molecules/ng RNA). Error bars, SEM for four independent experiments; numbers above bars, significant data for indicated days; gray, Mock; black, Aza.

(B) qRT-PCR of ERV genes in A2780 cells for four independent experiments. y axis, fold increases for Aza/Mock ± SEM and normalized to Mock = 1. White bars, non-significant; colored bars, significant ERV gene induction ($p < 0.05$).

(C) TASA-TD PCR amplified sense and antisense transcripts of the *env-Fc2* (731 bp) and *Syncytin-1* (202 bp) genes from first strand cDNA. Aza-treated A2780, Hey, and TykNu, and HCT116 and DKO cells are indicated. Ratios of sense (s) and antisense (as) determined by ImageJ. PCR primers, gene-specific (GS); TAG. β-actin sense 399 bp amplification product = negative control for as transcripts (Chen et al., 2004). The products from TASA-TD PCR were run on the same gel, then cropped and presented.

See also Figure S5.

IFI27, and *IFI44L*). The increases often exceeded that for the drug likely because total ERV RNA molecules were higher in the overexpression experiments (Figures S6F–S6I). Finally, although siRNA knockdown of individual ERVs (*Syncytin-1*, *ERV-3*) during Aza treatment produced more complex results, targeting two ERVs significantly blunted the Aza-induced gene expression of *IFI27*, *IFI44L*, and *IFI6* in TykNu cells, but not A2780 or Hey cells (Figure S7A).

Importantly, a driving role for ERV transcripts in triggering Aza-induced viral defense gene responses is evidenced by a high correlation of basal levels of both in 19 primary EOC. Total molecules of 22 ERV *env* genes queried were increased ($p < 0.05$) in tumor versus normal ($n = 9$) and divided tumors into lower ($n = 9$) and higher ERV ($n = 10$) expression groups as compared to normal controls. High ERV tumors had significantly higher viral defense response gene expression ($p = 0.000141$) (Figure 7A).

Viral Defense Gene Levels Divide Human Tumors into High and Low Expression Groups that Track with Responses to Immune Checkpoint Therapy

Human cancers can evolve immune evasion to become less responsive to immune modulation (Drake et al., 2006; Schreiber et al., 2011). In this regard, basal transcript levels for the Aza-induced viral defense genes grouped primary EOC, breast, colon, and lung cancers, and melanoma from The Cancer Genome Atlas (TCGA) studies into high and low groups (Figures 7B and S7C–S7F). For EOC, this basal expression divided tumors into high, medium, and low expression groups and the former two encompass virtually all of the TCGA (Verhaak et al., 2013) immune reactive (IMR) good prognosis tumors. The Low group encompasses the PRO (high proliferative), poor prognosis subtype ($p < 0.001$ to 0.0001) (Figures 7B and S7B). Interestingly, virtually all of the right-sided colon cancers with a high DNA hypermethylation frequency phenotype ($p < 0.002$), termed CIMP, which have a high

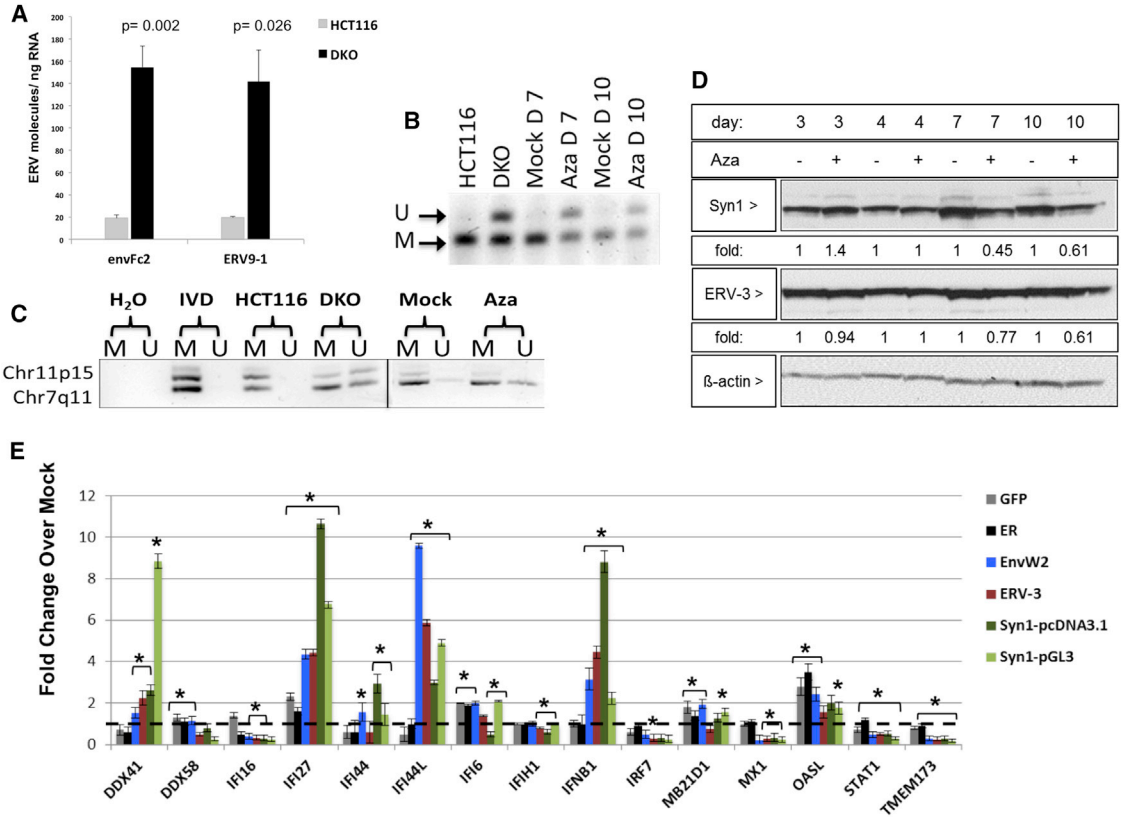

Figure 6. Aza Upregulates ERV Transcripts, but Not Proteins, through DNA Demethylation

(A) *env-Fc2* and *erv-9-1* ERV gene total number of molecules, assayed by qRT-PCR, for DKO (DNMT1$^{-/-}$, DNMT3B$^{-/-}$) and parental HCT116 cells. y axis, mean ± SEM for n = 6 biological replicates.

(B) DNA methylation changes in ERVs in A2780 cells treated with Mock or 500 nM Aza for 3 days at post-treatment day 4 (day 7) or 7 (day 10). Bisulfite-treated DNA was amplified and digested with the AciI enzyme producing 155 and 44 bp fragments of methylated DNA while unmethylated DNA does not digest (199 bp fragment). U, unmethylated band; M, methylated band.

(C) DNA from (B) was subjected to methylation-specific PCR for ERV-Fc2 family members on chromosomes 7 and 11. U, unmethylated; M, methylated; IVD, in vitro methylated DNA. The products from the same MSP reaction were run on two different gels and presented together. Vertical line indicates distinction between gels on the left and right.

(D) Syncytin-1 and ERV-3 protein levels in EOC cells treated as in (B). Fold change for densitometry by ImageJ for Aza versus Mock cells normalized to β-actin protein levels. The same gel blotted for Syncytin-1 and β-actin, then stripped and reprobed for ERV3. The space between the Syncytin-1 and ERV3 and the β-actin proteins was cropped out to conserve space.

(E) Transfection of full-length *env* genes from EnvW2, ERV-3, or Syncytin-1 or EGFP and ER controls in TykNu cells. qRT-PCR was performed for ISGs 7 days after transfection. Dotted black line indicates 1. Y axis, mean ± SEM fold change of three biological replicates for overexpression/Mock. *p $\leq$ 0.05.

See also Figure S6.

burden of DNA mutations and respond robustly to immune checkpoint therapy (Le et al., 2015), were in the High and Intermediate groups (Figure S7C). High mutation burden has recently been defined as a key correlate to response to immune checkpoint therapy (Rizvi et al., 2015; Snyder et al., 2014). Similar sharp high versus low clustering is seen for subgroups of breast and lung cancers and melanoma (Guan et al., 2015) (Figures S7D–S7F), the last being very responsive to immune checkpoint therapy (Topalian et al., 2015; Hodi et al., 2010; Weber et al., 2015).

Could the levels of viral defense pathway signaling correlate with improved responses to immune checkpoint therapy? Indeed, for RNA-seq transcriptomes of melanoma patients treated with anti-CTLA-4, high levels of the viral defense signature expression in tumor samples correlated with long term benefit (disease control [stable disease or better] >6 months as measured radiographically) in patients treated with anti-CTLA-4 therapy (Snyder et al., 2014) (Figures 7C and 7D; Tables S5 and S6). Importantly, high viral defense signature again correlated with high mutational burden (Figure 7C).

Aza Treatment Potentiates Immune Checkpoint Therapy in a Mouse Model of Melanoma

In the B16-F10 mouse melanoma model, multiple combinations of low dose Aza directly enhanced tumor responses to anti-CTLA4 immune checkpoint therapy (Figures 7E, 7F, and S7G). Further, B16 cells treated in vitro with Aza, then injected into mice and treated with anti-CTLA-4, were cleared completely (data not shown). Thus DNMTis can potentiate the anti-tumor effects of immune checkpoint inhibitors.

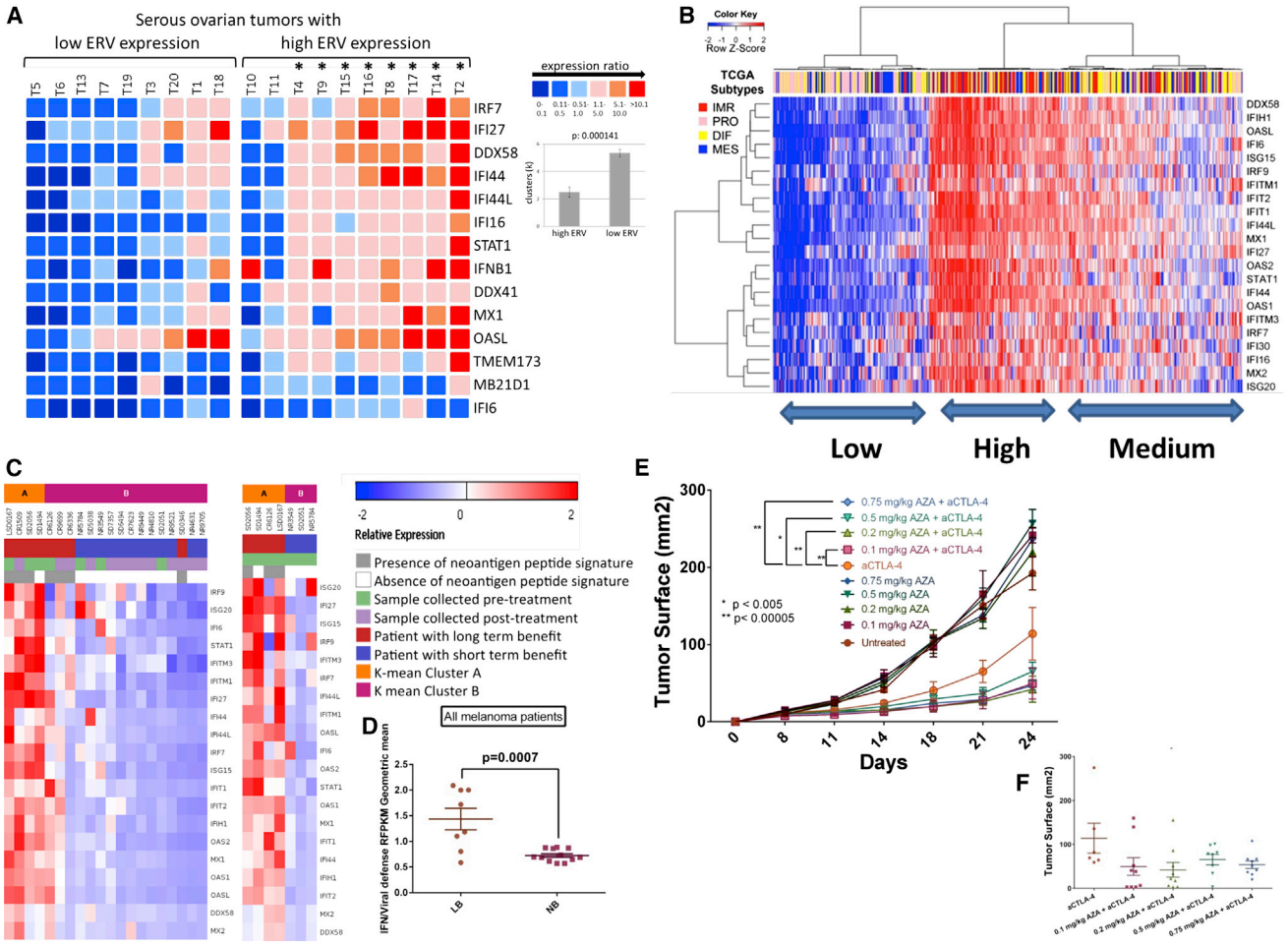

Figure 7. Aza-Upregulated Viral Defense Genes Are Significantly Correlated with ERVs in Primary Tumors and Correlate with Sensitivity to Immune Therapy

(A) Heatmap comparing basal levels of viral defense genes and ERVs in primary EOC. The cut-off for lower or higher ERVs was the mean control tissue value of 237.57 ± 83.05 molecules/ng RNA. Mean ISGs of the high ERV ovarian tumor (T) cohort (n = 10) is 12.65-fold higher than the mean of ISGs of the low ERV cohort (n = 9). The (*) denotes that eight of ten high ERV tumors had significantly higher ISG expression compared to the low ERV tumors. ISG expression is organized according to low and high ERV expression cohorts in arbitrary units; color code from blue to red shows increasing ISG expression. For clusters (k = 6), differences are significant between the high ERV expression (2.5 ± 0.37) and the low ERV expression cohort (5.33 ± 0.28).

(B) Interferon-stimulated viral defense genes upregulated at least 2-fold by Aza in EOC cell lines (right y axis) were used to cluster EOC tumors for RNA-seq data (blue, low; red, high) from The Cancer Genome Atlas (TCGA). EOC TCGA subtypes are shown: DIF (differentiated), IMR (immune reactive), MES (mesenchymal), and PRO (proliferative).

(C and D) Viral defense gene signature is upregulated in tumors from anti-CTLA-4-treated metastatic melanoma patients who derived durable clinical benefit (complete response, partial response, or progression free-survival >6 months as previously described) (Snyder et al., 2014) compared to those without benefit. Tumors collected pre-CTLA-4 treatment and shortly post-treatment are shown.

(D) y axis = RFPKM mean of viral defense genes in all melanoma patients.

(E and F) Tumor responses of mice injected with B16-F10 cells and treated with either PBS, anti-CTLA-4, Aza, or both anti-CTLA-4 and Aza. Data represent results from one of two independent experiments with identical results, each with n = 10 per arm. Y axis = mean tumor surface, error bars ± SEM.

See also Figure S7 and Tables S5 and S6.

DISCUSSION

Our present data now provide functional context for our earlier reports that DNMTis induce a complex set of immune pathway responses in tumor cells (Li et al., 2014; Wrangle et al., 2013). DNMTis trigger cytoplasmic dsRNA sensing, central to cellular viral defense responses, and activate interferon in EOC and colon cancer cells by disrupting DNMTs. This activation could induce tumor attraction of lymphocytes (Ivashkiv and Donlin, 2014). There are some important implications for one of the most exciting new developments in cancer treatment, immune checkpoint therapy (Brahmer et al., 2010, 2012; Berger et al., 2008; Leach et al., 1996; Topalian et al., 2015; Hodi et al., 2010; Weber et al., 2015) and for underlying mechanisms inherent to both tumor and host cells for reversal of immune tolerance in tumor infiltrating T-lymphocytes (Pardoll, 2012).

Indeed, basal levels of our viral defense gene transcripts divide EOC, and other major cancer types in TCGA, into low and high expression subgroups. Perhaps most intriguingly, such high basal expression in tumors tracks with favorable patient responses in a trial of immune checkpoint therapy for advanced melanoma, and strong Aza sensitization to immune checkpoint therapy is seen in a pre-clinical mouse melanoma model.

A major trigger of the Aza-induced viral defense response appears to be bidirectional transcription of ERVs that are known to fold into dsRNA secondary structures. ERVs, representing more than 8% of the human genome (Bannert and Kurth, 2004; Tristem, 2000), integrated into the genome of mammals between 0.1 and 40 million years ago via exogenous retroviral infections of germ cells (Egan et al., 2004; Turner et al., 2001). Most ERV genes are non-functional due to DNA recombination, mutations, and deletions, but some produce functional proteins including group-specific antigen (gag), polymerase (pol) with reverse transcriptase (RT), and the envelope (env) surface unit (SU) with a transmembrane immunosuppressive-like peptide (Mi et al., 2000; Blaise et al., 2005; de Parseval et al., 2003; Villesen et al., 2004). The *env* gene of *ERVW-1* (chromosome 7q21.2) called *Syncytin-1* has an essential role in placentogenesis (Blond et al., 1999; Mi et al., 2000).

Importantly, and key to our findings, a major function of DNA methylation in humans is silencing of ERVs and other viral sequences in the human genome; up to 90% of methylated CpGs are located in 45% of the human genome harboring repetitive elements like ERVs (Walsh et al., 1998; Bestor and Tycko, 1996). However, ERV genes are unmethylated and expressed in embryonic stem cells (Santoni et al., 2012) and especially *Syncytin-1* is epigenetically regulated throughout placentogenesis (Matousková et al., 2006). Some tumors have ERV demethylation and increased expression such as the ERV-K (HML-2) 5′LTR-UTR in melanoma (Stengel et al., 2010) and the 5′-LTR region of several ERVs in testicular cancer (Gimenez et al., 2010). A 20% overall mean demethylation of single CpGs in the ERVW-1 5′ LTR regulating *Syncytin-1* correlates with increased expression in endometrial cancer (Strissel et al., 2012). Indeed, ERVs can be targeted as tumor-associated antigens on melanoma cells (Cooper et al., 2015). In contrast, as in our present data and those of others (Maksakova et al., 2008), in some cancers, individual ERVs can maintain full or partial promoter DNA methylation and low expression and DNMTis can induce ERV demethylation and viral defense signaling in human embryonic stem cells (Grow et al., 2015).

In addition to ERVs, other noncoding RNAs could contribute to the Aza-induced immune response, such as repetitive Alu elements (Tarallo et al., 2012). UV light can damage small nucleolar RNA and activate an interferon response via TLR3 (Bernard et al., 2012) and very high dose (10 μM) Dac can induce an interferon response, apoptosis, increased ERVs and repetitive satellite RNAs in p53 null mouse fibroblasts (Leonova et al., 2013). We suspect, however, that such high Dac doses induce DNA damage rather than simply epigenetic effects. Half of the ovarian cancer lines we studied (Li et al., 2014) have wild-type *P53* but we see no differences in Aza interferon response between these and those with mutant *P53*.

The high translational connotations of our findings, including the small number of patients in clinical trials for NSCLC who may have been sensitized by epigenetic priming to immune therapy (Wrangle et al., 2013), remain to be validated in larger clinical trials. These are ongoing for NSCLC (Brahmer, 2015) and planned for advanced ovarian cancer. Moreover, ERV-K env proteins have been shown to increase immunotherapeutic potential of melanoma, breast, and ovarian cancer patients (Rycaj et al., 2015; Wang-Johanning et al., 2012; Cooper et al., 2015). Also, our hypotheses that drugs like Aza might sensitize patients with multiple cancer types to immune checkpoint blockade and other immunotherapies are further strengthened by the data in our pre-clinical melanoma model. For immune checkpoint therapy, in addition to the functional significance of our data, a potential biomarker strategy is suggested by our findings in a melanoma trial. The high correlation of viral defense signaling with mutational burden suggests that genetic changes, increases in ERVs, and viral defense genes could predict response to immune checkpoint and other immunomodulatory approaches. Finally, our drug approach to upregulate viral defense signaling might be compared to the use of oncolytic viruses to induce inflammatory immune infiltrates at tumor sites to sensitize to immunomodulation (Zamarin et al., 2014).

EXPERIMENTAL PROCEDURES

Detailed materials and methods can be found in the Supplemental Experimental Procedures.

Cell Line Treatments

Cell lines were treated with 500 nM Aza, 100 nM Dac, or 500 nM-3 μM carboplatin (Sigma) for 72 hr, and DNA and RNA were isolated using standard methods at 1, 3, or 7 days following removal of drug. Ruxolitinib (2 μM) (Invivogen tlrl-rux), 0.625–5 U/ml of anti-IFNAR2 antibody (PBL Interferon Source 21385-1), 0.625–2.5 U/ml of anti-IFNB antibody (PBL Interferon Source 31400-1), or 1.25–5 U/ml of anti-IL10RB antibody (Abcam ab89884) were added during DNMTi treatment. Preparation of nuclear and cytoplasmic fractions of cultured cells was performed as described (O'Hagan et al., 2011). Ribosomal RNA was depleted using the Ribominus kit (Invitrogen), and PolyA$^+$ and PolyA$^-$ RNA were isolated using the Oligotex Direct mRNA Mini Kit (Invitrogen). Nucleic acids were treated with 1 U/μg of RNase III (Ambion), 10 U/μg of RNaseH (Invitrogen), or 3 U/1 μg calf intestine alkaline phosphatase (New England Biolabs) according to manufacturer's instructions, and 400 ng of each nucleic acid was transfected into HT29 cells.

DNA Methylation Analysis

DNA was bisulfite converted and subjected to methylation-specific PCR (Herman et al., 1996) for *IRF7* and *ERV-Fc2* and COBRA (Xiong and Laird, 1997) for the *ERV-Fc2* locus on chromosome 11.

Transcript Abundance

Real-time RT-PCR was performed with an Applied Biosystems 7500 Fast Real-Time PCR machine by the $2^{-\Delta\Delta CT}$ method and TASA-TD strand-specific PCR by the method of Henke et al. (2015).

Protein Analysis

Western blot analyses employed antibodies against ERV-3 (1:1,000, Everest), B-actin (1:5,000, Sigma), MDA5 (1:1,000, Cell Signaling 5321), PARP (9542, 1:1,000; Cell Signaling Technology), RIG-I (1:1,000, Cell Signaling 4200), STING (1:1,000, Abcam ab82960), Syncytin-1 (1:350, Dr. Hervé Perron, Geneuro, Geneva Switzerland), and TLR3 (1:1,000, Cell Signaling 6961). IFNB

ELISA utilized the *Verikine-HS* Human Interferon Beta Serum ELISA kit (PBL Interferon Source) and IFNL ELISA the DuoSet ELISA for Human IL-29/IL28-B (IFNL 1/3) kit (R&D Systems).

Knockdown and Overexpression Experiments

Syncytin-1, *ERV-3* and *ERV-W2 env*, *Estrogen receptor alpha (ER)*, and E-GFP vectors and siRNAs targeting Syncytin-1, ERV-3, or a scrambled control, were transfected using the JetPei or Hyperfect transfection reagents, respectively. TLR3, MAVS, and STING shRNA were performed according to established methods (Stewart et al., 2003).

RNA-Seq Expression Analysis of Tumors from Anti-CTLA-4-Treated Patients

Patients were described previously (Snyder et al., 2014) and samples were obtained with written informed consent per approved institutional review board (IRB) protocols. Expression data were obtained using RNA-seq with all data deposited at The cBio portal under the study name Metastatic Melanoma (MSKCC Cell, 2015).

B16-F10 Melanoma Mouse Model

C57BL/6J mice were subcutaneously injected with 1×10^5 B16-F10 tumor cells. On days 4, 8, 11, 14, and 18, mice were treated intraperitoneally with 100 μg anti-ctla-4. Mice received two cycles of intraperitoneal injection of 0.1 to 0.75 mg/kg Aza in PBS for 5 consecutive days followed by 7 days off treatment, starting at day 8 after developing palpable tumors, with control groups receiving corresponding doses of non-specific isotype antibody control and PBS intraperitoneally. Tumor surface was measured with a caliper using the ellipse surface formula (length × width × π)/400. All mouse procedures were performed in accordance with the institutional protocol guidelines from the Memorial Sloan Kettering Cancer Center (New York, NY).

Statistical Analysis

Mean ± SEM qRT-PCR results were considered statistically significant with p values ≤ 0.05 by Mann-Whitney U test or Student's t tests and two-tailed p values are reported. Tumor growth was assessed by two-way ANOVA between each of the mouse treatment groups with p values adjusted by the Dunnett multiple comparison test (df = 512).

Normalized, level 3 Agilent expression data were obtained from The Cancer Genome Atlas data portal (https://tcga-data.nci.nih.gov/tcga/) and analyzed by R statistical software (http://www.r-project.org) with existing packages and customized routines. Consensus hierarchical clustering was performed with the ConsensusClusterPlus R-package (Wilkerson and Hayes, 2010) and data analyzed by the Fisher exact p value test for association between clusters.

ACCESSION NUMBERS

The expression data reported in this paper is deposited in dbGaP via accession number phs001038.

SUPPLEMENTAL INFORMATION

Supplemental Information includes Supplemental Experimental Procedures, seven figures, and six tables and can be found with this article online at http://dx.doi.org/10.1016/j.cell.2015.07.011.

AUTHOR CONTRIBUTIONS

K.B.C., P.L.S., A.D., T.M., J.W., T.A.C., S.B.B., and R.S. designed experiments, performed data analyses, and wrote the manuscript. K.B.C., P.L.S., C.H., A.D., A.H., B.A., and S.B. performed experiments. N.S.R. provided ERV-3 *env* cDNA plasmid. D.S. provided ovarian cancer cell lines. H.L., A.S., V.M., D.M.P., L.M.C., M.W.B., and C.A.Z. assisted with data analyses.

ACKNOWLEDGMENTS

Research was supported by grants from The National Cancer Institute (NCI) CA058184 (S.B.B.), Stand Up To Cancer (SU2C) Epigenetic Dream Team (S.B.B.), the Hodson Trust (S.B.B.), the Samuel Waxman Cancer Research Foundation (S.B.B.), The Dr. Miriam and Sheldon G. Adelson Medical Research Foundation (S.B.B., D.J.S.), Department of Defense (DOD) Teal Award BC031272 (S.B.B.), the Pershing Square Sohn Cancer Research Alliance (T.A.C.), the STARR Cancer Consortium (T.A.C.), the Ludwig Foundation (J.D.W.), and NIH award F32CA183214 (K.B.C.), and German Cancer Aid (Deutsche Krebshilfe 108215) (R.S.). We acknowledge Mrs. Elizabeth Stiegler and Florentine Koppitz for their expert technical help and Kathy Bender for manuscript preparation. ABI TLDA qRT-PCR was conducted at the Genetic Resources Core Facility, Johns Hopkins Institute of Genetic Medicine, Baltimore, MD. We thank Ms. Jennifer Meyers and the Next Generation Sequencing Center at the Sidney Kimmel Comprehensive Cancer Center for Agilent Bioanalyzer analysis. D.M.P. is a consultant for Pfizer and Amplimmune. J.D.W. is a consultant for Bristol-Myers Squibb and receives research funding. S.B.B. consults for MDxHealth. Methylation-specific PCR (MSP) is licensed to MDxHealth in agreement with Johns Hopkins University (JHU), and S.B.B. and JHU are entitled to royalty shares received from sales.

Received: December 19, 2014
Revised: May 4, 2015
Accepted: June 26, 2015
Published: August 27, 2015; corrected online February 25, 2016

REFERENCES

Anglesio, M.S., Wiegand, K.C., Melnyk, N., Chow, C., Salamanca, C., Prentice, L.M., Senz, J., Yang, W., Spillman, M.A., Cochrane, D.R., et al. (2013). Type-specific cell line models for type-specific ovarian cancer research. PLoS ONE *8*, e72162.

Bannert, N., and Kurth, R. (2004). Retroelements and the human genome: new perspectives on an old relation. Proc. Natl. Acad. Sci. USA *101* (*Suppl 2*), 14572–14579.

Baylin, S.B., and Jones, P.A. (2011). A decade of exploring the cancer epigenome - biological and translational implications. Nat. Rev. Cancer *11*, 726–734.

Bénit, L., Calteau, A., and Heidmann, T. (2003). Characterization of the low-copy HERV-Fc family: evidence for recent integrations in primates of elements with coding envelope genes. Virology *312*, 159–168.

Berger, R., Rotem-Yehudar, R., Slama, G., Landes, S., Kneller, A., Leiba, M., Koren-Michowitz, M., Shimoni, A., and Nagler, A. (2008). Phase I safety and pharmacokinetic study of CT-011, a humanized antibody interacting with PD-1, in patients with advanced hematologic malignancies. Clin. Cancer Res. *14*, 3044–3051.

Bernard, J.J., Cowing-Zitron, C., Nakatsuji, T., Muehleisen, B., Muto, J., Borkowski, A.W., Martinez, L., Greidinger, E.L., Yu, B.D., and Gallo, R.L. (2012). Ultraviolet radiation damages self noncoding RNA and is detected by TLR3. Nat. Med. *18*, 1286–1290.

Bestor, T.H., and Tycko, B. (1996). Creation of genomic methylation patterns. Nat. Genet. *12*, 363–367.

Blaise, S., de Parseval, N., and Heidmann, T. (2005). Functional characterization of two newly identified Human Endogenous Retrovirus coding envelope genes. Retrovirology *2*, 19.

Blond, J.L., Besème, F., Duret, L., Bouton, O., Bedin, F., Perron, H., Mandrand, B., and Mallet, F. (1999). Molecular characterization and placental expression of HERV-W, a new human endogenous retrovirus family. J. Virol. *73*, 1175–1185.

Brahmer, J. (2015). Phase II Anti-PD1 Epigenetic Priming Study in NSCLC (NA_00084192). https://clinicaltrials.gov/ct2/show/NCT01928576.

Brahmer, J.R., Drake, C.G., Wollner, I., Powderly, J.D., Picus, J., Sharfman, W.H., Stankevich, E., Pons, A., Salay, T.M., McMiller, T.L., et al. (2010). Phase I study of single-agent anti-programmed death-1 (MDX-1106) in refractory

solid tumors: safety, clinical activity, pharmacodynamics, and immunologic correlates. J. Clin. Oncol. *28*, 3167–3175.

Brahmer, J.R., Tykodi, S.S., Chow, L.Q., Hwu, W.J., Topalian, S.L., Hwu, P., Drake, C.G., Camacho, L.H., Kauh, J., Odunsi, K., et al. (2012). Safety and activity of anti-PD-L1 antibody in patients with advanced cancer. N. Engl. J. Med. *366*, 2455–2465.

Chen, J., Sun, M., Kent, W.J., Huang, X., Xie, H., Wang, W., Zhou, G., Shi, R.Z., and Rowley, J.D. (2004). Over 20% of human transcripts might form sense-antisense pairs. Nucleic Acids Res. *32*, 4812–4820.

Chiappinelli, K.B., Haynes, B.C., Brent, M.R., and Goodfellow, P.J. (2012). Reduced DICER1 elicits an interferon response in endometrial cancer cells. Mol. Cancer Res. *10*, 316–325.

Cooper, L.J., Krishnamurthy, J., Rabinovich, B., Mi, T., Switzer, K., Olivares, S., Maiti, S., Plummer, J.B., Singh, H., Kumaresan, P., et al. (2015). Genetic engineering of T cells to target HERV-K, an ancient retrovirus on melanoma. Clin. Cancer Res. *21*, 3241–3251.

de Parseval, N., Lazar, V., Casella, J.F., Benit, L., and Heidmann, T. (2003). Survey of human genes of retroviral origin: identification and transcriptome of the genes with coding capacity for complete envelope proteins. J. Virol. *77*, 10414–10422.

Ding, S., and Robek, M.D. (2014). Peroxisomal MAVS activates IRF1-mediated IFN-λ production. Nat. Immunol. *15*, 700–701.

Ding, S., Khoury-Hanold, W., Iwasaki, A., and Robek, M.D. (2014). Epigenetic reprogramming of the type III interferon response potentiates antiviral activity and suppresses tumor growth. PLoS Biol. *12*, e1001758.

Domcke, S., Sinha, R., Levine, D.A., Sander, C., and Schultz, N. (2013). Evaluating cell lines as tumour models by comparison of genomic profiles. Nat. Commun. *4*, 2126.

Drake, C.G., Jaffee, E., and Pardoll, D.M. (2006). Mechanisms of immune evasion by tumors. Adv. Immunol. *90*, 51–81.

Egan, M.F., Straub, R.E., Goldberg, T.E., Yakub, I., Callicott, J.H., Hariri, A.R., Mattay, V.S., Bertolino, A., Hyde, T.M., Shannon-Weickert, C., et al. (2004). Variation in GRM3 affects cognition, prefrontal glutamate, and risk for schizophrenia. Proc. Natl. Acad. Sci. USA *101*, 12604–12609.

Faghihi, M.A., Modarresi, F., Khalil, A.M., Wood, D.E., Sahagan, B.G., Morgan, T.E., Finch, C.E., St Laurent, G., 3rd, Kenny, P.J., and Wahlestedt, C. (2008). Expression of a noncoding RNA is elevated in Alzheimer's disease and drives rapid feed-forward regulation of beta-secretase. Nat. Med. *14*, 723–730.

Gimenez, J., Montgiraud, C., Pichon, J.P., Bonnaud, B., Arsac, M., Ruel, K., Bouton, O., and Mallet, F. (2010). Custom human endogenous retroviruses dedicated microarray identifies self-induced HERV-W family elements reactivated in testicular cancer upon methylation control. Nucleic Acids Res. *38*, 2229–2246.

Grow, E.J., Flynn, R.A., Chavez, S.L., Bayless, N.L., Wossidlo, M., Wesche, D.J., Martin, L., Ware, C.B., Blish, C.A., Chang, H.Y., et al. (2015). Intrinsic retroviral reactivation in human preimplantation embryos and pluripotent cells. Nature *522*, 221–225.

Guan, J., Gupta, R., and Filipp, F.V. (2015). Cancer systems biology of TCGA SKCM: efficient detection of genomic drivers in melanoma. Sci. Rep. *5*, 7857.

Henke, C., Strissel, P.L., Schubert, M.-T., Mitchell, M., Stolt, C.C., Faschingbauer, F., Beckmann, M.W., and Strick, R. (2015). Selective expression of sense and antisense transcripts of the sushi-ichi-related retrotransposon–derived family during mouse placentogenesis. Retrovirology *12*, 9.

Herman, J.G., Graff, J.R., Myöhänen, S., Nelkin, B.D., and Baylin, S.B. (1996). Methylation-specific PCR: a novel PCR assay for methylation status of CpG islands. Proc. Natl. Acad. Sci. USA *93*, 9821–9826.

Hodi, F.S., O'Day, S.J., McDermott, D.F., Weber, R.W., Sosman, J.A., Haanen, J.B., Gonzalez, R., Robert, C., Schadendorf, D., Hassel, J.C., et al. (2010). Improved survival with ipilimumab in patients with metastatic melanoma. N. Engl. J. Med. *363*, 711–723.

Hurst, T., and Magiorkinis, G. (2014). Activation of the innate immune response by endogenous retroviruses. J. Gen. Virol. *96*, 1207–1218.

Ivashkiv, L.B., and Donlin, L.T. (2014). Regulation of type I interferon responses. Nat. Rev. Immunol. *14*, 36–49.

Issa, J.P. (2005). Optimizing therapy with methylation inhibitors in myelodysplastic syndromes: dose, duration, and patient selection. Nat. Clin. Pract. Oncol. *2* (*Suppl 1*), S24–S29.

James, S.R., Cedeno, C.D., Sharma, A., Zhang, W., Mohler, J.L., Odunsi, K., Wilson, E.M., and Karpf, A.R. (2013). DNA methylation and nucleosome occupancy regulate the cancer germline antigen gene MAGEA11. Epigenetics *8*, 849–863.

Juergens, R.A., Wrangle, J., Vendetti, F.P., Murphy, S.C., Zhao, M., Coleman, B., Sebree, R., Rodgers, K., Hooker, C.M., Franco, N., et al. (2011). Combination epigenetic therapy has efficacy in patients with refractory advanced non-small cell lung cancer. Cancer Discov. *1*, 598–607.

Kaminskas, E., Farrell, A., Abraham, S., Baird, A., Hsieh, L.S., Lee, S.L., Leighton, J.K., Patel, H., Rahman, A., Sridhara, R., et al.; FDA (2005). Approval summary: azacitidine for treatment of myelodysplastic syndrome subtypes. Clin. Cancer Res. *11*, 3604–3608.

Karikó, K., Buckstein, M., Ni, H., and Weissman, D. (2005). Suppression of RNA recognition by Toll-like receptors: the impact of nucleoside modification and the evolutionary origin of RNA. Immunity *23*, 165–175.

Karpf, A.R., Peterson, P.W., Rawlins, J.T., Dalley, B.K., Yang, Q., Albertsen, H., and Jones, D.A. (1999). Inhibition of DNA methyltransferase stimulates the expression of signal transducer and activator of transcription 1, 2, and 3 genes in colon tumor cells. Proc. Natl. Acad. Sci. USA *96*, 14007–14012.

Karpf, A.R., Lasek, A.W., Ririe, T.O., Hanks, A.N., Grossman, D., and Jones, D.A. (2004). Limited gene activation in tumor and normal epithelial cells treated with the DNA methyltransferase inhibitor 5-aza-2′-deoxycytidine. Mol. Pharmacol. *65*, 18–27.

Karpf, A.R., Bai, S., James, S.R., Mohler, J.L., and Wilson, E.M. (2009). Increased expression of androgen receptor coregulator MAGE-11 in prostate cancer by DNA hypomethylation and cyclic AMP. Mol. Cancer Res. *7*, 523–535.

Kulaeva, O.I., Draghici, S., Tang, L., Kraniak, J.M., Land, S.J., and Tainsky, M.A. (2003). Epigenetic silencing of multiple interferon pathway genes after cellular immortalization. Oncogene *22*, 4118–4127.

Larsen, J.M., Christensen, I.J., Nielsen, H.J., Hansen, U., Bjerregaard, B., Talts, J.F., and Larsson, L.I. (2009). Syncytin immunoreactivity in colorectal cancer: potential prognostic impact. Cancer Lett. *280*, 44–49.

Laska, M.J., Nissen, K.K., and Nexø, B.A. (2013). (Some) cellular mechanisms influencing the transcription of human endogenous retrovirus, HERV-Fc1. PLoS ONE *8*, e53895.

Le, D.T., Uram, J.N., Wang, H., Bartlett, B.R., Kemberling, H., Eyring, A.D., Skora, A.D., Luber, B.S., Azad, N.S., Laheru, D., et al. (2015). PD-1 blockade in tumors with mismatch-repair deficiency. N. Engl. J. Med. *372*, 2509–2520.

Leach, D.R., Krummel, M.F., and Allison, J.P. (1996). Enhancement of antitumor immunity by CTLA-4 blockade. Science *271*, 1734–1736.

Leonova, K.I., Brodsky, L., Lipchick, B., Pal, M., Novototskaya, L., Chenchik, A.A., Sen, G.C., Komarova, E.A., and Gudkov, A.V. (2013). p53 cooperates with DNA methylation and a suicidal interferon response to maintain epigenetic silencing of repeats and noncoding RNAs. Proc. Natl. Acad. Sci. USA *110*, E89–E98.

Li, H., Chiappinelli, K.B., Guzzetta, A.A., Easwaran, H., Yen, R.W., Vatapalli, R., Topper, M.J., Luo, J., Connolly, R.M., Azad, N.S., et al. (2014). Immune regulation by low doses of the DNA methyltransferase inhibitor 5-azacitidine in common human epithelial cancers. Oncotarget *5*, 587–598.

Löwer, R., Löwer, J., Tondera-Koch, C., and Kurth, R. (1993). A general method for the identification of transcribed retrovirus sequences (R-U5 PCR) reveals the expression of the human endogenous retrovirus loci HERV-H and HERV-K in teratocarcinoma cells. Virology *192*, 501–511.

Maksakova, I.A., Mager, D.L., and Reiss, D. (2008). Keeping active endogenous retroviral-like elements in check: the epigenetic perspective. Cell. Mol. Life Sci. *65*, 3329–3347.

Mankan, A.K., Schmidt, T., Chauhan, D., Goldeck, M., Höning, K., Gaidt, M., Kubarenko, A.V., Andreeva, L., Hopfner, K.P., and Hornung, V. (2014). Cytosolic RNA:DNA hybrids activate the cGAS-STING axis. EMBO J. *33*, 2937–2946.

Matei, D., Fang, F., Shen, C., Schilder, J., Arnold, A., Zeng, Y., Berry, W.A., Huang, T., and Nephew, K.P. (2012). Epigenetic resensitization to platinum in ovarian cancer. Cancer Res. *72*, 2197–2205.

Matousková, M., Blazková, J., Pajer, P., Pavlícek, A., and Hejnar, J. (2006). CpG methylation suppresses transcriptional activity of human syncytin-1 in non-placental tissues. Exp. Cell Res. *312*, 1011–1020.

Mi, S., Lee, X., Li, X., Veldman, G.M., Finnerty, H., Racie, L., LaVallie, E., Tang, X.Y., Edouard, P., Howes, S., et al. (2000). Syncytin is a captive retroviral envelope protein involved in human placental morphogenesis. Nature *403*, 785–789.

O'Hagan, H.M., Wang, W., Sen, S., Destefano Shields, C., Lee, S.S., Zhang, Y.W., Clements, E.G., Cai, Y., Van Neste, L., Easwaran, H., et al. (2011). Oxidative damage targets complexes containing DNA methyltransferases, SIRT1, and polycomb members to promoter CpG Islands. Cancer Cell *20*, 606–619.

Odunsi, K., Matsuzaki, J., James, S.R., Mhawech-Fauceglia, P., Tsuji, T., Miller, A., Zhang, W., Akers, S.N., Griffiths, E.A., Miliotto, A., et al. (2014). Epigenetic potentiation of NY-ESO-1 vaccine therapy in human ovarian cancer. Cancer Immunol. Res. *2*, 37–49.

Pardoll, D.M. (2012). The blockade of immune checkpoints in cancer immunotherapy. Nat. Rev. Cancer *12*, 252–264.

Platanias, L.C. (2005). Mechanisms of type-I- and type-II-interferon-mediated signalling. Nat. Rev. Immunol. *5*, 375–386.

Rizvi, N.A., Hellmann, M.D., Snyder, A., Kvistborg, P., Makarov, V., Havel, J.J., Lee, W., Yuan, J., Wong, P., Ho, T.S., et al. (2015). Cancer immunology. Mutational landscape determines sensitivity to PD-1 blockade in non-small cell lung cancer. Science *348*, 124–128.

Robek, M.D., Boyd, B.S., and Chisari, F.V. (2005). Lambda interferon inhibits hepatitis B and C virus replication. J. Virol. *79*, 3851–3854.

Rote, N.S., Chakrabarti, S., and Stetzer, B.P. (2004). The role of human endogenous retroviruses in trophoblast differentiation and placental development. Placenta *25*, 673–683.

Ruebner, M., Strissel, P.L., Ekici, A.B., Stiegler, E., Dammer, U., Goecke, T.W., Faschingbauer, F., Fahlbusch, F.B., Beckmann, M.W., and Strick, R. (2013). Reduced syncytin-1 expression levels in placental syndromes correlates with epigenetic hypermethylation of the ERVW-1 promoter region. PLoS ONE *8*, e56145.

Rycaj, K., Plummer, J.B., Yin, B., Li, M., Garza, J., Radvanyi, L.G., Ramondetta, L.M., Lin, K., Johanning, G.L., Tang, D.G., et al. (2015). Cytotoxicity of human endogenous retrovirus K-specific T cells toward autologous ovarian cancer cells. Clin. Cancer Res. *21*, 471–483.

Santoni, F.A., Guerra, J., and Luban, J. (2012). HERV-H RNA is abundant in human embryonic stem cells and a precise marker for pluripotency. Retrovirology *9*, 111.

Schaefer, M., Hagemann, S., Hanna, K., and Lyko, F. (2009). Azacytidine inhibits RNA methylation at DNMT2 target sites in human cancer cell lines. Cancer Res. *69*, 8127–8132.

Schreiber, R.D., Old, L.J., and Smyth, M.J. (2011). Cancer immunoediting: integrating immunity's roles in cancer suppression and promotion. Science *331*, 1565–1570.

Sistigu, A., Yamazaki, T., Vacchelli, E., Chaba, K., Enot, D.P., Adam, J., Vitale, I., Goubar, A., Baracco, E.E., Remédios, C., et al. (2014). Cancer cell-autonomous contribution of type I interferon signaling to the efficacy of chemotherapy. Nat. Med. *20*, 1301–1309.

Snyder, A., Makarov, V., Merghoub, T., Yuan, J., Zaretsky, J.M., Desrichard, A., Walsh, L.A., Postow, M.A., Wong, P., Ho, T.S., et al. (2014). Genetic basis for clinical response to CTLA-4 blockade in melanoma. N. Engl. J. Med. *371*, 2189–2199.

Stengel, S., Fiebig, U., Kurth, R., and Denner, J. (2010). Regulation of human endogenous retrovirus-K expression in melanomas by CpG methylation. Genes Chromosomes Cancer *49*, 401–411.

Stewart, S.A., Dykxhoorn, D.M., Palliser, D., Mizuno, H., Yu, E.Y., An, D.S., Sabatini, D.M., Chen, I.S., Hahn, W.C., Sharp, P.A., et al. (2003). Lentivirus-delivered stable gene silencing by RNAi in primary cells. RNA *9*, 493–501.

Stresemann, C., Brueckner, B., Musch, T., Stopper, H., and Lyko, F. (2006). Functional diversity of DNA methyltransferase inhibitors in human cancer cell lines. Cancer Res. *66*, 2794–2800.

Strick, R., Ackermann, S., Langbein, M., Swiatek, J., Schubert, S.W., Hashemolhosseini, S., Koscheck, T., Fasching, P.A., Schild, R.L., Beckmann, M.W., and Strissel, P.L. (2007). Proliferation and cell-cell fusion of endometrial carcinoma are induced by the human endogenous retroviral Syncytin-1 and regulated by TGF-beta. J. Mol. Med. *85*, 23–38.

Strissel, P.L., Ruebner, M., Thiel, F., Wachter, D., Ekici, A.B., Wolf, F., Thieme, F., Ruprecht, K., Beckmann, M.W., and Strick, R. (2012). Reactivation of codogenic endogenous retroviral (ERV) envelope genes in human endometrial carcinoma and prestages: emergence of new molecular targets. Oncotarget *3*, 1204–1219.

Su, W.Y., Li, J.T., Cui, Y., Hong, J., Du, W., Wang, Y.C., Lin, Y.W., Xiong, H., Wang, J.L., Kong, X., et al. (2012). Bidirectional regulation between WDR83 and its natural antisense transcript DHPS in gastric cancer. Cell Res. *22*, 1374–1389.

Sun, L., Wu, J., Du, F., Chen, X., and Chen, Z.J. (2013). Cyclic GMP-AMP synthase is a cytosolic DNA sensor that activates the type I interferon pathway. Science *339*, 786–791.

Tarallo, V., Hirano, Y., Gelfand, B.D., Dridi, S., Kerur, N., Kim, Y., Cho, W.G., Kaneko, H., Fowler, B.J., Bogdanovich, S., et al. (2012). DICER1 loss and Alu RNA induce age-related macular degeneration via the NLRP3 inflammasome and MyD88. Cell *149*, 847–859.

Topalian, S.L., Hodi, F.S., Brahmer, J.R., Gettinger, S.N., Smith, D.C., McDermott, D.F., Powderly, J.D., Carvajal, R.D., Sosman, J.A., Atkins, M.B., et al. (2012). Safety, activity, and immune correlates of anti-PD-1 antibody in cancer. N. Engl. J. Med. *366*, 2443–2454.

Topalian, S.L., Drake, C.G., and Pardoll, D.M. (2015). Immune checkpoint blockade: a common denominator approach to cancer therapy. Cancer Cell *27*, 450–461.

Tristem, M. (2000). Identification and characterization of novel human endogenous retrovirus families by phylogenetic screening of the human genome mapping project database. J. Virol. *74*, 3715–3730.

Tsai, H.C., Li, H., Van Neste, L., Cai, Y., Robert, C., Rassool, F.V., Shin, J.J., Harbom, K.M., Beaty, R., Pappou, E., et al. (2012). Transient low doses of DNA-demethylating agents exert durable antitumor effects on hematological and epithelial tumor cells. Cancer Cell *21*, 430–446.

Turner, G., Barbulescu, M., Su, M., Jensen-Seaman, M.I., Kidd, K.K., and Lenz, J. (2001). Insertional polymorphisms of full-length endogenous retroviruses in humans. Curr. Biol. *11*, 1531–1535.

Verhaak, R.G., Tamayo, P., Yang, J.Y., Hubbard, D., Zhang, H., Creighton, C.J., Fereday, S., Lawrence, M., Carter, S.L., Mermel, C.H., et al. (2013). Prognostically relevant gene signatures of high-grade serous ovarian carcinoma. J. Clin. Invest. *123*, 517–525.

Villesen, P., Aagaard, L., Wiuf, C., and Pedersen, F.S. (2004). Identification of endogenous retroviral reading frames in the human genome. Retrovirology *1*, 32.

Walsh, C.P., Chaillet, J.R., and Bestor, T.H. (1998). Transcription of IAP endogenous retroviruses is constrained by cytosine methylation. Nat. Genet. *20*, 116–117.

Wang-Johanning, F., Frost, A.R., Johanning, G.L., Khazaeli, M.B., LoBuglio, A.F., Shaw, D.R., and Strong, T.V. (2001). Expression of human endogenous retrovirus k envelope transcripts in human breast cancer. Clin. Cancer Res. *7*, 1553–1560.

Wang-Johanning, F., Frost, A.R., Jian, B., Epp, L., Lu, D.W., and Johanning, G.L. (2003). Quantitation of HERV-K env gene expression and splicing in human breast cancer. Oncogene *22*, 1528–1535.

Wang-Johanning, F., Liu, J., Rycaj, K., Huang, M., Tsai, K., Rosen, D.G., Chen, D.T., Lu, D.W., Barnhart, K.F., and Johanning, G.L. (2007). Expression of multiple human endogenous retrovirus surface envelope proteins in ovarian cancer. Int. J. Cancer *120*, 81–90.

Wang-Johanning, F., Rycaj, K., Plummer, J.B., Li, M., Yin, B., Frerich, K., Garza, J.G., Shen, J., Lin, K., Yan, P., et al. (2012). Immunotherapeutic potential of anti-human endogenous retrovirus-K envelope protein antibodies in targeting breast tumors. J. Natl. Cancer Inst. *104*, 189–210.

Weber, J.S., D'Angelo, S.P., Minor, D., Hodi, F.S., Gutzmer, R., Neyns, B., Hoeller, C., Khushalani, N.I., Miller, W.H., Jr., Lao, C.D., et al. (2015). Nivolumab versus chemotherapy in patients with advanced melanoma who progressed after anti-CTLA-4 treatment (CheckMate 037): a randomised, controlled, open-label, phase 3 trial. Lancet Oncol. *16*, 375–384.

Wilkerson, M.D., and Hayes, D.N. (2010). ConsensusClusterPlus: a class discovery tool with confidence assessments and item tracking. Bioinformatics *26*, 1572–1573.

Wrangle, J., Wang, W., Koch, A., Easwaran, H., Mohammad, H.P., Vendetti, F., Vancriekinge, W., Demeyer, T., Du, Z., Parsana, P., et al. (2013). Alterations of immune response of non-small cell lung cancer with azacytidine. Oncotarget *4*, 2067–2079.

Xiong, Z., and Laird, P.W. (1997). COBRA: a sensitive and quantitative DNA methylation assay. Nucleic Acids Res. *25*, 2532–2534.

Zamarin, D., Holmgaard, R.B., Subudhi, S.K., Park, J.S., Mansour, M., Palese, P., Merghoub, T., Wolchok, J.D., and Allison, J.P. (2014). Localized oncolytic virotherapy overcomes systemic tumor resistance to immune checkpoint blockade immunotherapy. Sci. Transl. Med. *6*, 226ra32.